JCI The Journal of Clinical Investigation

von Willebrand factor mutation promotes thrombocytopathy by inhibiting integrin αIIbβ3

Caterina Casari, … , Cécile V. Denis, Marijke Bryckaert

J Clin Invest. 2013;123(12):5071-5081. https://doi.org/10.1172/JCI69458.

Research Article

von Willebrand disease type 2B (vWD-type 2B) is characterized by gain-of-function mutations in von Willebrand factor (vWF) that enhance its binding to the glycoprotein Ib-IX-V complex on platelets. Patients with vWD-type 2B have a bleeding tendency that is linked to loss of vWF multimers and/or thrombocytopenia. In this study, we uncovered evidence that platelet dysfunction is a third possible mechanism for bleeding tendency. We found that platelet aggregation, secretion, and spreading were diminished due to inhibition of integrin αIIbβ3 in platelets from mice expressing a vWD-type 2B–associated vWF (vWF/p.V1316M), platelets from a patient with the same mutation, and control platelets pretreated with recombinant vWF/p.V1316M. Impaired platelet function coincided with reduced thrombus growth. Further, αIIbβ3 activation and activation of the small GTPase Rap1 were impaired by vWF/p.V1316M following exposure to platelet agonists (thrombin, ADP, or convulxin). Conversely, thrombin- or ADP-induced Ca^{2+} store release, which is required for αIIbβ3 activation, was normal, indicating that vWF/p.V1316M acts downstream of Ca^{2+} release and upstream of Rap1. We found normal Syk phosphorylation and PLCγ2 activation following collagen receptor signaling, further implying that vWF/p.V1316M acts directly on or downstream of Ca^{2+} release. These data indicate that the vWD-type 2B mutation p.V1316M is associated with severe thrombocytopathy, which likely contributes to the bleeding tendency in vWD-type 2B.

von Willebrand factor mutation promotes thrombocytopathy by inhibiting integrin αIIbβ3

Caterina Casari,[1,2] Eliane Berrou,[1,2] Marilyne Lebret,[1,2] Frédéric Adam,[1,2] Alexandre Kauskot,[1,2] Régis Bobe,[1,2] Céline Desconclois,[2,3] Edith Fressinaud,[1,2] Olivier D. Christophe,[1,2] Peter J. Lenting,[1,2] Jean-Philippe Rosa,[1,2] Cécile V. Denis,[1,2] and Marijke Bryckaert[1,2]

[1]INSERM U770, Le Kremlin Bicêtre, France. [2]Université Paris-Sud, Le Kremlin Bicêtre, France.
[3]Service Hématologie Biologique, Assistance Publique–Hôpitaux de Paris, Le Kemlin Bicêtre, France.

von Willebrand disease type 2B (vWD-type 2B) is characterized by gain-of-function mutations in von Willebrand factor (vWF) that enhance its binding to the glycoprotein Ib-IX-V complex on platelets. Patients with vWD-type 2B have a bleeding tendency that is linked to loss of vWF multimers and/or thrombocytopenia. In this study, we uncovered evidence that platelet dysfunction is a third possible mechanism for bleeding tendency. We found that platelet aggregation, secretion, and spreading were diminished due to inhibition of integrin αIIbβ3 in platelets from mice expressing a vWD-type 2B–associated vWF (vWF/p.V1316M), platelets from a patient with the same mutation, and control platelets pretreated with recombinant vWF/p.V1316M. Impaired platelet function coincided with reduced thrombus growth. Further, αIIbβ3 activation and activation of the small GTPase Rap1 were impaired by vWF/p.V1316M following exposure to platelet agonists (thrombin, ADP, or convulxin). Conversely, thrombin- or ADP-induced Ca^{2+} store release, which is required for αIIbβ3 activation, was normal, indicating that vWF/p.V1316M acts downstream of Ca^{2+} release and upstream of Rap1. We found normal Syk phosphorylation and PLCγ2 activation following collagen receptor signaling, further implying that vWF/p.V1316M acts directly on or downstream of Ca^{2+} release. These data indicate that the vWD-type 2B mutation p.V1316M is associated with severe thrombocytopathy, which likely contributes to the bleeding tendency in vWD-type 2B.

Introduction

von Willebrand factor (vWF) is a multimeric glycoprotein present in platelets, megakaryocytes, plasma, and endothelial cells, the latter being the primary source of circulating vWF (1, 2). vWF is essential for primary hemostasis. Indeed, initial platelet adhesion to the subendothelium following endothelial damage is mediated via interactions between vWF and the platelet glycoprotein Ib-IX-V (GPIb-IX-V) receptor complex. Furthermore, vWF interacts with integrin αIIbβ3, which is required for stable adhesion and for platelet-platelet interactions under high-shear stress conditions (1).

The fundamental role of vWF in hemostasis is illustrated in patients with von Willebrand disease (vWD) who exhibit a bleeding tendency. This bleeding disorder is classified into 3 major types. Type 1 and type 3 are characterized by quantitative deficiencies (partial [type 1] and virtually complete [type 3] deficiencies), whereas type 2 results from qualitative defects (3). vWD-type 2B is characterized by gain-of-function mutations in the vWF A1 domain, which comprises the binding site for GPIbα (4, 5). In vWD-type 2B, the clinical outcome is strongly dependent on the mutation (5, 6). The bleeding phenotype in vWD-type 2B is often explained by (a) the absence of high-molecular-weight vWF multimers, the most functionally effective forms; (b) the unavailability of GPIbα, due to constitutively bound 2B mutants; and (c) the moderate to severe thrombocytopenia observed in these patients. Thrombocytopenia may originate from impaired platelet production (7) and/or from the incorporation of platelets into circulating vWF/platelets aggregates (8). The possibility that a potentially impaired platelet function in vWD-type 2B contributes to the bleeding phenotype has attracted little attention. A single study published 25 years ago showed that reduced platelet aggregation and secretion were correlated to impaired granule contents in response to thrombin, collagen, and ADP in 2 patients with vWD-type 2B (9). Along the same line, an in vitro study using perfusion assays on a collagen matrix reported a heterogeneous defect in thrombus growth in vWD-type 2B (10).

To investigate whether abnormal platelet function participates in the bleeding tendency of patients with vWD-type 2B, we undertook a comprehensive, step-by-step functional analysis of platelets isolated from a patient with the severe vWD-type 2B mutation vWF/p.V1316M and of control platelets pretreated with recombinant vWF/pV1316M. In addition, we examined platelets isolated from a mouse expressing vWF carrying the same mutation (11).

We now report that the vWD-type 2B mutation vWF/p.V1316M induces a severe defect in platelet activation. Spreading, aggregation, and secretion were strongly diminished in platelets isolated from mice expressing vWF/p.V1316M or from a patient harboring the p.V1316M vWF mutation or in control platelets in the presence of recombinant vWF/p.V1316M. These defects were correlated with an almost complete defect in αIIbβ3 integrin activation. Impaired platelet function was associated with reduced thrombus growth under flow. Mechanistic studies in the absence of secreted ADP reveal that Rap1 activity, as induced by GPCRs or by the collagen-receptor GPVI and which is required for αIIbβ3 activation, was impaired. Since Ca^{2+} store release, an upstream signaling step, was normal, this strongly suggests that vWF/p.V1316M acts between Ca^{2+} store release and Rap1. Altogether, our results indicate that constitutive binding of vWF/p.V1316M to platelets severely disturbs the signaling pathways required for αIIbβ3 activation, demonstrating that vWD-type

Authorship note: Caterina Casari and Eliane Berrou contributed equally to this work.

Conflict of interest: The authors have declared that no conflict of interest exists.

Citation for this article: *J Clin Invest.* 2013;123(12):5071–5081. doi:10.1172/JCI69458.

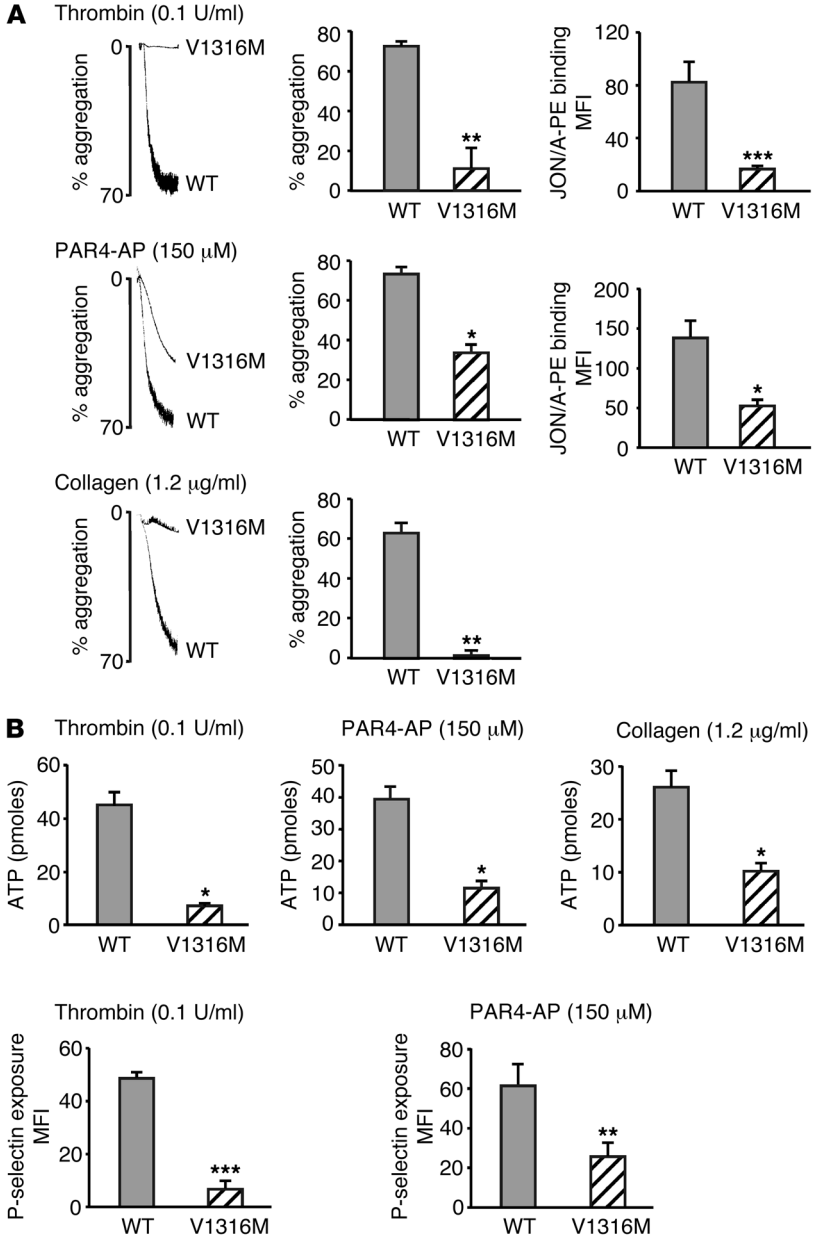

Figure 1

Platelet aggregation, secretion, and αIIbβ3 integrin activation in mvWF/p.V1316M. (**A**) Aggregation and integrin αIIbβ3 activation of washed platelets were initiated by adding thrombin (0.1 U/ml), PAR4-AP (150 μM), and collagen (1.2 μg/ml). Aggregation was expressed as the percentage change in light transmission, with the value for the blank (buffer without platelet) set at 100%. Traces are representative of 3 independent experiments. Integrin αIIbβ3 activation was assessed by flow cytometry. Platelets were incubated with a phycoerythrin-labeled rat anti-mouse integrin αIIbβ3 mAb (JON/A) specific for the activated conformation of the mouse integrin. Flow cytometry was performed without stirring. The level of activated integrin is indicated by the MFI ± SEM from at least 3 experiments. (**B**) Dense and α granule secretion were assessed by measuring ATP release and P-selectin exposure, respectively. ATP was quantified after platelet aggregation induced by various agonists (thrombin, PAR4-AP, collagen) and expressed as the amount of ATP released (pmoles). P-selectin exposure was evaluated by flow cytometry using FITC-labeled rat anti-mouse P-selectin mAb. The level of P-selectin exposed at the surface is expressed as MFI ± SEM from at least 3 experiments. $^{*}P < 0.05$; $^{**}P < 0.01$; $^{***}P < 0.001$ (paired Student's *t* test).

2B mutations induce a thrombocytopathy likely to contribute to the bleeding phenotype associated with this disorder.

Results

Platelet aggregation, secretion, and spreading are altered in mice expressing mvWF/p.V1316M. We first used our mouse model for vWD-type 2B (11) to examine the effect of the vWF/p.V1316M mutation on platelet aggregation, integrin αIIbβ3 activation, and platelet secretion induced by various agonists. Platelets were isolated from mice expressing murine vWF/p.V1316M (mvWF/p.V1316M) or control mice expressing WT murine vWF (WT-mvWF). The former mice were previously shown to exhibit vWD-type 2B features, including prolonged tail bleeding time and thrombocytopenia (11). Interestingly, aggregation of mvWF/p.V1316M mouse platelets was either absent or severely decreased (56%) when induced by various agonists (Figure 1A). Since aggregation requires integrin αIIbβ3 activation, we next evaluated the activation level of integrin αIIbβ3 by use of JON/A, a mAb specific for the activated conformation of mouse integrin αIIbβ3. Using flow cytometry, the level of JON/A binding to integrin αIIbβ3 after stimulation with thrombin (0.1 U/ml) was 80% lower in mvWF/p.V1316M-derived platelets than in WT-mvWF–derived platelets (Figure 1A). A 62.2% decrease in JON/A binding was also observed when mvWF/p.V1316M platelets were activated by protease-activated receptor agonist peptides (PAR4-AP) (150 μM) (Figure 1A).

We next quantified dense granule and α granule secretion by measuring ATP release and by detecting P-selectin exposure, respectively. After 3 minutes of incubation with low-dose thrombin (0.1 U/ml), PAR4-AP (150 μM), or collagen (1.2 μg/ml) under stirring conditions, ATP release from dense granules was decreased by 70%, 73%, and 61%,

Table 1
Clinical and laboratory parameters of the patient with vWD-type 2B

Mutation	p.Val1316Met
Sex	M
Bleeding score	14
PFA-100 Epi and ADP (s)	>300
Platelet count (10^9/l)	40
Mean platelet volume (fl)	15
FVIII:C (U/dl)	62
vWF:Ag (U/dl)	67
vWF:RCo (U/dl)	22
vWF multimers	Complete loss of HMW; partial loss of intermediate MW

Epi, epinephrine; HMW, high molecular weight; FVII:C, procoagulant activity of FVIII; vWF:Ag, vWF antigen; vWF:RCo, vWF ristocetin cofactor activity.

respectively, in mvWF/p.V1316M-derived platelets compared with that in WT-mvWF–derived platelets (Figure 1B). P-selectin exposure, as evaluated by flow cytometry in unstirred platelets and as stimulated by thrombin (0.1 U/ml) or PAR4-AP (150 μM), was 86% and 58% lower in mvWF/p.V1316M-derived platelets than in WT-mvWF–derived platelets, respectively. Altogether, these results demonstrate that the mvWF/p.V1316M mutation affects platelet aggregation, integrin αIIbβ3 activation, and platelet secretion.

Next, platelet spreading on fibrinogen was investigated. Platelets stimulated with thrombin (0.1–0.5 U/ml) or PAR4-AP (100–200 μM) were immediately deposited on fibrinogen-coated (100 μg/ml) coverslips and incubated for 30 minutes. Thrombin or PAR4-AP increased WT-mvWF platelet spreading surface area almost 2 fold, from 1.34 ± 0.06 μm^2 to 2.49 ± 0.08 μm^2 (85 % increase) or to 2.17 ± 0.06 μm^2 (78% increase), respectively (Supplemental Figure 1; supplemental material available online with this article; doi:10.1172/JCI69458DS1). Interestingly, platelet surface area increased significantly less during spreading of mvWF/p.V1316M-derived platelets: only 64% (from 1.32 ± 0.04 μm^2 to 2.17 ± 0.05 μm^2 [$P < 0.01$ vs. WT]) for thrombin and 34% (from 1.24 ± 0.03 μm^2 to 1.62 ± 0.05 μm^2 [$P < 0.05$ vs. WT]) for PAR4-AP. Our results demonstrate a lower platelet spreading of mvWF/p.V1316M-derived murine platelets on fibrinogen, consistent with altered cytoskeletal reorganization.

Platelets from a patient carrying the vWF/p.V1316M mutation are functionally impaired. Next, we examined the activation of human platelets from a patient with vWD-type 2B carrying the vWF/p.V1316M mutation. The patient exhibited a low platelet count (40×10^9 platelets per l), a severe bleeding tendency (Table 1), and the presence of large platelets and small aggregates (Supplemental Figure 2). The level of receptors (αIIbβ3, 140%; β1, 123%; GPIbα, 163%, GPVI, 194%) (Figure 2, A and B) was increased and was correlated with increased platelet volume (Table 1). Likewise, α granule content was also increased (vWF, 146%; PF4, 154%) (Figure 2, A–C), contrasting with a previous work showing that α granule content was partially impaired in patients with vWD-type 2B (9).

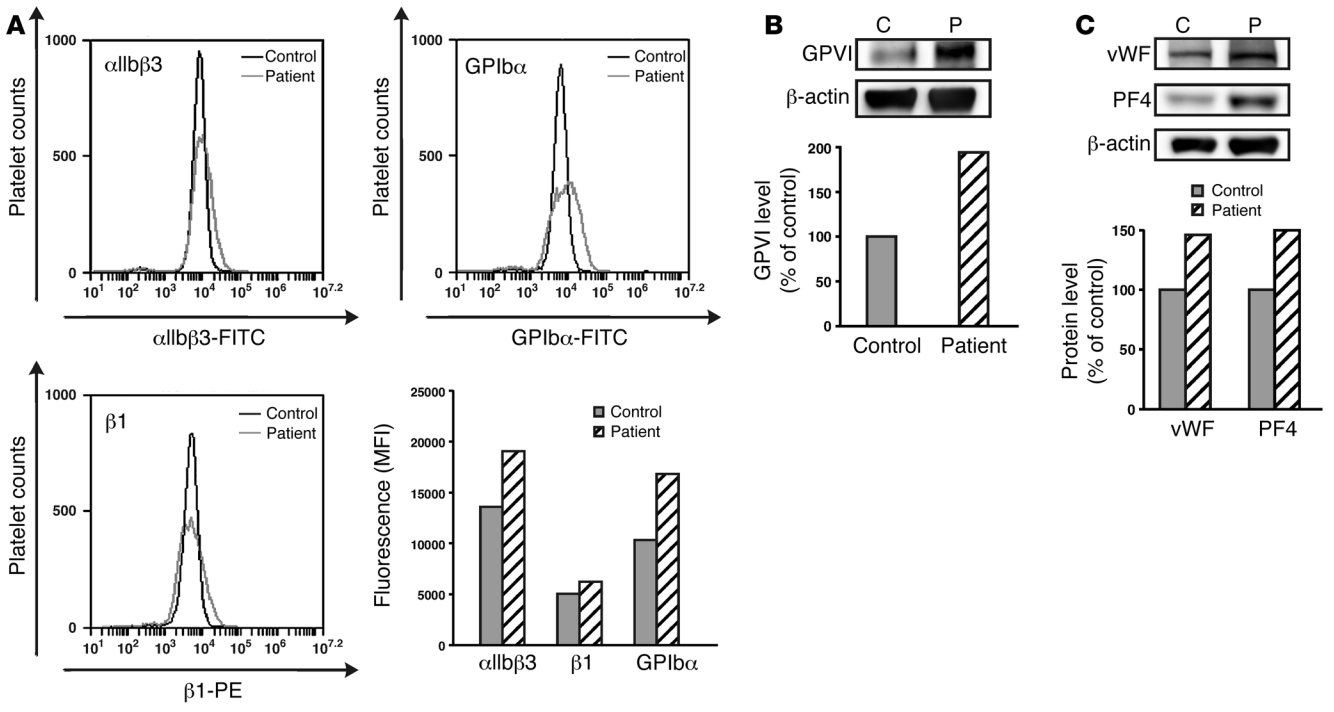

Figure 2
Analysis of adhesive receptors and granule contents of platelets from a patient with vWD-type 2B exhibiting the vWF/p.V1316M mutation. (**A** and **B**) The expression of adhesive receptors was analyzed by flow cytometry or immunoblotting. (**A**) Control and patient platelet suspensions were incubated with antibodies directed against αIIbβ3 (HIP8) and α2β1 (MAR4) integrins or against GPIbα (HIP1). Antibody binding was assessed by flow cytometry. (**B**) GPVI expression was quantified by immunoblotting. (**C**) α Granule content was assessed by immunoblotting with an anti-vWF and an anti-PF4. Results are representative of 2 independent experiments.

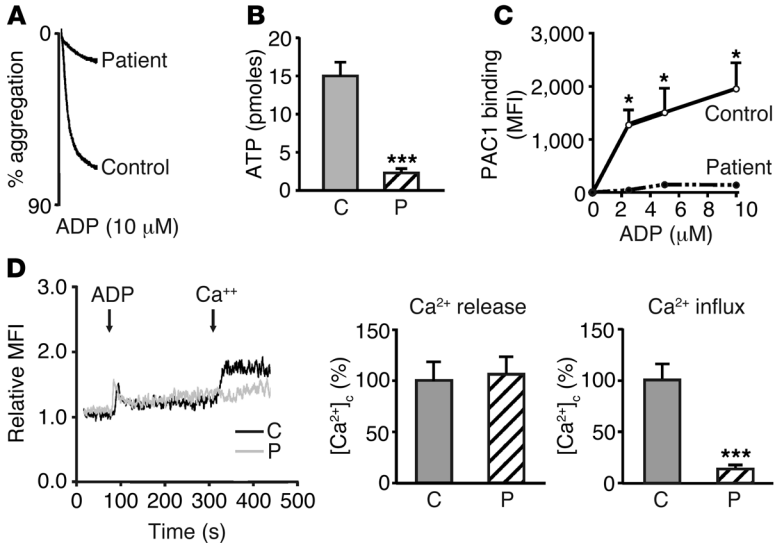

Figure 3
ADP-induced activation of platelets from the patient with vWD-type 2B. Control and patient platelet suspensions were stimulated with various concentrations of ADP. (**A**) Aggregation of washed platelets was initiated by adding 10 μM ADP. (**B**) Dense granule secretion was assessed by measuring the amount of ATP release (pmoles). C, control donor; P, patient. (**C**) Integrin αIIbβ3 activation was assessed by flow cytometry using integrin αIIbβ3 mAb (PAC1) specific for the activated conformation of the human integrin. The level of activated integrin is indicated by MFI. (**D**) Ca^{2+} signaling induced by 10 μM ADP was monitored by flow cytometry using the Oregon Green 488 BAPTA1-AM. Histograms represent the area under the curve of both Ca^{2+} store release and Ca^{2+} influx. Data from 1 experiment carried out in triplicate are presented as mean ± SEM. *$P < 0.05$; ***$P < 0.001$ (unpaired Student's *t* test). Results are representative of 2 independent experiments.

Next, we examined aggregation, secretion, and activation of integrin αIIbβ3. Platelet aggregation and secretion induced by ADP (10 μM) or thrombin (0.1–0.5 U/ml) were drastically decreased (Figure 3, A and B, and Figure 4A, respectively). Note that the mildly elevated platelet secretion observed in control platelets upon stimulation with ADP was probably the result of a slight platelet activation after letting blood settle for 2 hours at room temperature, a procedure to maximize recovery of large platelets from the patient (see Methods). In parallel, the binding of PAC1 was also abolished (7% of control), consistent with diminished αIIbβ3 activation (Figure 3C). A similar decrease was also found in platelet aggregation induced by thrombin in the presence of the ADP scavenger apyrase (Figure 4B), indicating that the defect lay in both ADP- and thrombin-specific signaling pathways. These results show that the vWD-type 2B p.V1316M mutation is associated with a marked alteration of platelet αIIbβ3 engagement. To approach the mechanism at play, we next examined the corresponding signaling pathways, i.e., Ca^{2+} signaling elicited by GPCR receptors (P2Y1 or PARs) acting through phospholipase β (PLCβ) activity. Ca^{2+} store release, which is required for αIIbβ3 activation (12), was unaffected (Figure 3D and Figure 4C, respectively). Altogether, these results show that vWF/p.V1316M interferes with the αIIbβ3 inside-out signaling pathway downstream of Ca^{2+} store release.

Contrasting with normal Ca^{2+} store release, the Ca^{2+} influx was totally abolished in the patient's platelets (Figure 3D and Figure 4C, respectively). Ca^{2+} influx is not involved in αIIbβ3 activation but is involved in thrombus stability (12), suggesting that, in addition to αIIbβ3 activation, vWF/p.V1316M interferes with other pathways involved in thrombus stability.

The collagen receptor GPVI represents the other major activation pathway for platelet activation. We thus examined the effect of the vWF/p.V1316M mutation on GPVI signaling after stimulation with the potent GPVI agonist convulxin (Cvx). Platelet aggregation and secretion induced by Cvx (0.5–5 nM), whether in the absence or in the presence of apyrase, were impaired (Figure 5, A and B). The difference in platelet aggregation of the patient's platelets in the presence or absence of apyrase was statistically not significant. These results indicate that vWF/p.V1316M also inhibits the GPVI signaling pathway. This pathway involves the phosphorylation of the Syk tyrosine kinase, followed by that of its substrate, PLCγ2, which both appeared normal (Figure 5C). The downstream signaling events, Ca^{2+} store release and Ca^{2+} influx, were assessed: Ca^{2+} store release was only moderately altered (61% ± 10% of control, $P = 0.03$), while Ca^{2+} influx was severely diminished (18% ± 7% of control, $P < 0.001$) (Figure 5D). Altogether, these results indicate that human vWF/p.V1316M (hvWF/p.V1316M) strongly inhibits αIIbβ3 activation and aggregation via GPVI signaling. Similar to P2Y and PAR receptors pathways, hvWF/p.V1316M operates mainly downstream of Ca^{2+} store release. Additionally, Ca^{2+} influx was also severely affected, suggesting altered thrombus stability.

Next, we assessed the impact of the p.V1316M mutation on thrombus formation. For these experiments, reconstituted blood with normalized platelet counts was perfused on a collagen matrix. After 5 minutes of perfusion at 300 s^{-1}, homogeneous thrombi were observed using control blood. In contrast, the patient's platelets formed strings on the collagen matrix (Figure 6A). The surface area covered by the patient's platelets was only slightly decreased compared with that of control platelets (78% ± 6% of control), but the integrated fluorescence intensity, representative of thrombus growth, was considerably diminished, down to 16% ± 1% of that of control platelets. Since the p.V1316M mutation is known to affect vWF interactions with GPIbα, we extended our study to a shear rate of 1,500 s^{-1}. After 2 minutes at 1,500 s^{-1}, the control platelets formed thrombi, whereas the patient's platelets only developed individual platelet adhesion (Figure 6B). The percentage of surface covered by the patient's platelets was normal (94% ± 2%), as opposed to strongly decreased thrombi formation (as measured by integrated fluorescence intensity), down to 26% ± 9% of that of control platelets (arbitrarily set at 100%). These data are consistent with a defect in collagen-induced thrombus formation in the platelets from the patient with vWD-type 2B carrying the V1316M mutation and with the altered engagement of αIIbβ3 observed in aggregation assays.

Recombinant hvWF/p.V1316M mutation induces aggregation and signaling defects in control platelets. To check the direct effect of hvWF/p.V1316M on platelet functions, control platelets were pretreated with recombinant hvWF/p.V1316M before activation. First, as assessed by flow cytometry, vWF/p.V1316M bound efficiently to

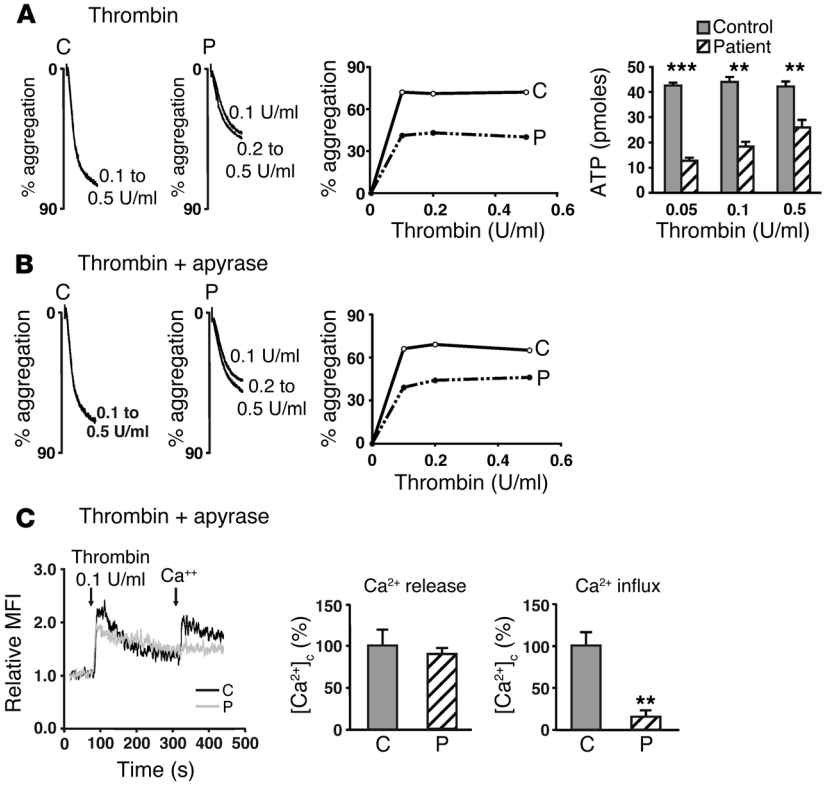

Figure 4

Thrombin-induced activation of platelets from the patient with vWD-type 2B. Washed platelets from a control donor and the patient with vWF/p.V1316M mutation were stimulated with thrombin in the (**A**) absence or (**B** and **C**) presence of apyrase (2 U/ml). (**A**) Aggregation and secretion of washed platelets were initiated by adding various concentrations of thrombin (0.1–0.5 U/ml). Dense granule secretion was assessed by measuring the amount of ATP release (pmoles). (**C**) Thrombin-induced Ca^{2+} signaling was monitored by flow cytometry using Oregon Green 488 BAPTA1-AM. Histograms represent the area under the curve of both the Ca^{2+} store release and Ca^{2+} influx. Data from 1 experiment carried out in triplicate are presented as mean ± SEM. $^{**}P < 0.01$; $^{***}P < 0.001$ (unpaired Student's *t* test). Results are representative of 2 independent experiments.

unstimulated platelets as opposed to control vWF (Figure 7). Pretreatment with an antibody specific for GPIbα (SZ2) (13) inhibited vWF/pV1316M binding. Altogether, these results clearly show that recombinant vWF/p.V1316M binds to GPIb-IX-V.

Next, human control platelets were preincubated for 10 minutes with various concentrations of recombinant hvWF/p.V1316M before addition of ADP (10 μM). Using PAC1 and flow cytometry, activation of integrin αIIbβ3 was totally abolished (0% of control) (Figure 8A). To confirm these results, platelet aggregation was performed with different concentrations of ADP. No ADP aggregation was observed in the presence of mutated vWF, whatever the concentration used (5–40 μM) (Figure 8B). Additionally, hvWF/WT and hvWF/p.V1316M did not trigger any dense granule secretion (Figure 8C). Similar to that for the platelets from the patient with vWD-type 2B, Ca^{2+} store release was normal after 5 minutes of ADP stimulation (Figure 8D). Surprisingly, in contrast to that in the patient's platelets, Ca^{2+} influx was unaffected. Likewise, Akt phosphorylation (Akt-P) was normal (Figure 8E), showing that PI3 kinase β activity, depending upon the P2Y12 ADP receptor (14), was not affected. Thus, the block in αIIbβ3 activation induced by vWF/p.V1316M binding to platelets occurs downstream of Ca^{2+} store release. Importantly, the activation of the small GTPase Rap1 (Rap1-GTP), which is dependent on Ca^{2+} store release and is required for αIIbβ3 activation, was totally abrogated when control platelets pretreated with hvWF/p.V1316M were stimulated with ADP (Figure 8F). This finding is consistent with the absence of PAC1 binding and thus of αIIbβ3 activation (Figure 8A). Altogether, these results confirm data obtained with the platelets from the patient with vWD-type 2B and mice exhibiting vWF/p.V1316M and show that vWF/p.V1316M inhibits platelet aggregation and αIIbβ3 activation by interfering with the regulation of Rap1 downstream of Ca^{2+} store release. The reason for the discrepancy in Ca^{2+} influx between the patient's platelets and recombinant vWF/pV1316M bound control platelets is unclear but may originate from a specific intrinsic defect of the patient's platelets.

Similar results were obtained with other GPCR agonists, including thrombin, PAR1-AP, and PAR4-AP. Recombinant vWF/p.V1316M inhibits platelet aggregation, secretion, and αIIbβ3 induced by thrombin (Supplemental Figure 3), PAR1-AP, and PAR4-AP (Supplemental Figure 4) by interfering downstream of Ca^{2+} mobilization and upstream of Rap1. Altogether, these results confirm the data obtained with the patient's platelets and that vWF/p.V1316M inhibits platelet aggregation and secretion induced by GPCRs through both ADP and thrombin receptor pathways.

Finally, we examined the effect of vWF/p.V1316M on the GPVI signaling pathway after stimulation with Cvx and also with collagen. First, platelet aggregation and secretion induced by Cvx (0.5–10 nM) (Figure 9A) or collagen (1–5 μg/ml) (Supplemental Figure 5) were partially or totally impaired in the presence of recombinant hvWF/p.V1316M. In the presence of apyrase, recombinant hvWF/p.V1316M impaired platelet aggregation induced by Cvx (Figure 9B) and collagen (Supplemental Figure 5), confirming that vWF/p.V1316M also interferes with the GPVI signaling pathway. Activation of αIIbβ3 was assessed at various concentrations of Cvx in the presence of hvWF/p.V1316M and apyrase. In these conditions, PAC1 binding was totally abolished (Figure 9C), demonstrating that the inside-out signaling pathway induced by GPVI was affected. Phosphorylation of Syk and PLCγ2 was normal in the presence of hvWF/p.V1316M and apyrase (Figure 9D), and, downstream of PLCγ2, Ca^{2+} store release and Ca^{2+} influx were also normal regardless of the concentration of Cvx (Figure 9E). Finally, in the presence of recombinant vWF/p.V1316M and of the antagonists of

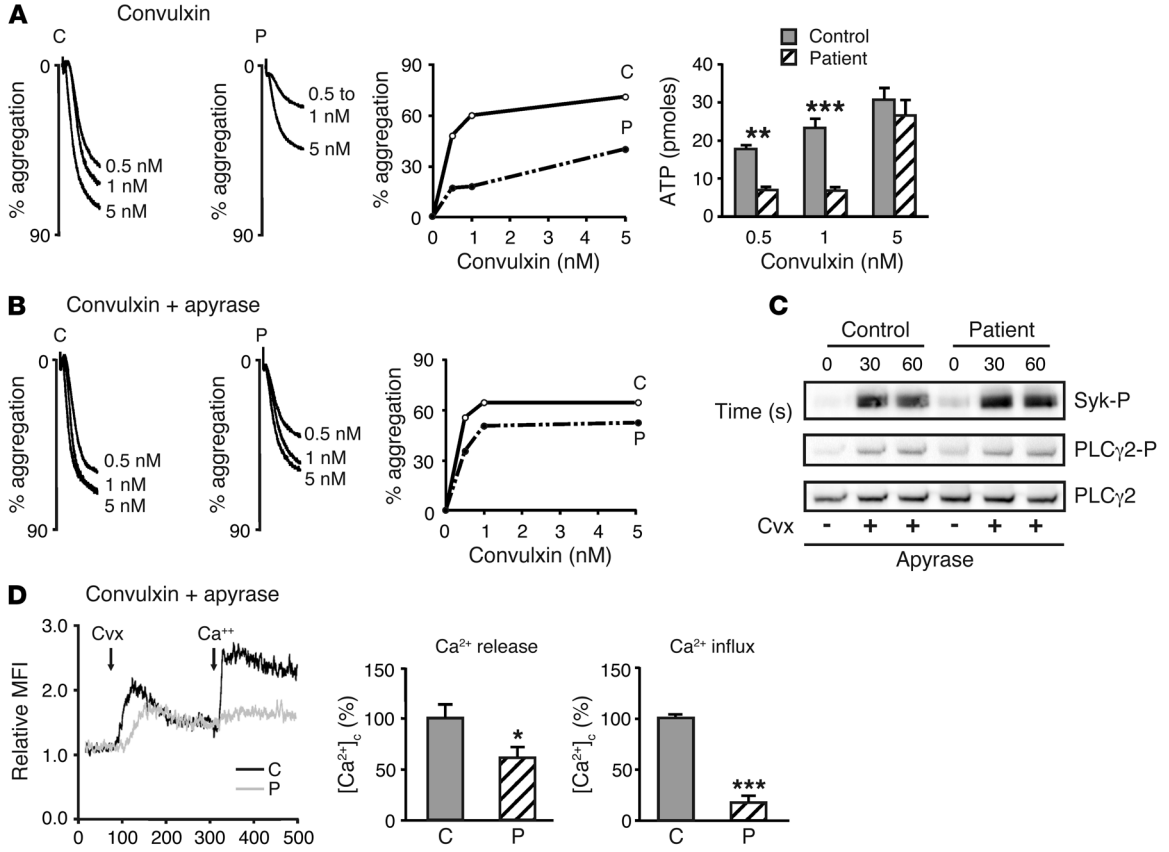

Figure 5

Cvx-induced activation of platelets from the patient with vWD-type 2B. Washed platelets from a control donor and patient with vWF/p.V1316M mutation were stimulated with Cvx in the (**A**) absence or (**B**–**D**) presence of apyrase (2 U/ml). Aggregation and secretion of washed platelets were initiated by adding various concentrations of Cvx (0.5–5 nM). Dense granule secretion was assessed by measuring the amount of ATP release (pmoles). (**C**) Washed platelets in suspension were activated by 5 nM Cvx for 30 and 60 seconds in the absence of stirring, and then tyrosine phosphorylation of Syk (Syk-P) and PLCγ2 (PLCγ2-P) was assessed by immunoblotting with an anti–Syk-P and anti–PLCγ2-P, respectively. (**D**) Ca^{2+} signaling induced by 5 nM Cvx was monitored by flow cytometry using the Oregon Green 488 BAPTA1-AM. Histograms represent the area under the curve of both the Ca^{2+} store release and Ca^{2+} influx. Data from 1 experiment carried out in triplicate are presented as mean ± SEM. $^*P = 0.03$; $^{**}P < 0.01$; $^{***}P < 0.001$ (unpaired Student's *t* test). Results are representative of 2 independent experiments.

P2Y1 and P2Y12 receptors, a marked inhibition of Rap1 activity was observed (Figure 9F), consistent with inhibition of αIIbβ3 activation (Figure 9C). Altogether, these results confirm that vWF/p.V1316M alters GPVI signaling, as it does for ADP and thrombin signaling pathways, by acting downstream of normal Ca^{2+} store release and upstream of Rap1 and blunting αIIbβ3 activation. Taken as a whole, our results indicate that vWF/p.V1316M inhibits αIIbβ3 activation at a converging point of the major ADP-, thrombin- and GPVI-dependent activation pathways downstream of Ca^{2+} store release, i.e., Rap1 activation, whether assessed in the mouse model of vWF/p.V1316M, in control platelets in the presence of vWF/p.V1316M, or, most importantly, in the platelets of a patient with vWD-type 2B carrying the vWF/p.V1316M mutation.

Discussion

vWD-type 2B can be particularly challenging in terms of treatment options. DDAVP is usually contraindicated, since by releasing the abnormal protein, it may only worsen the clinical picture (15). In addition, the accompanying exaggerated thrombocytopenia is associated with an increase in disease severity, leading to the need for concomitant platelet transfusions and vWF replacement therapy. Whether platelets themselves are abnormal or not in vWD-type 2B has not been addressed thoroughly so far. An early case report of 2 related patients with vWD-type 2B mentioned altered platelet aggregation associated with impaired granule contents (vWF and PF-4) but without conclusive evidence that the observed defects were in fact related to the vWD-type 2B status. The presence of giant platelets in some patients with vWD-type 2B (7) may also be consistent with suboptimal platelet functions. A recent study showed that mice with platelet counts greater 10% of controls displayed normal hemostasis (16), suggesting that thrombocytopenia is probably not the only cause of the bleeding phenotype observed in patients and mice with vWD-type 2B. Finally, the idea that the abnormal interaction of vWF with GPIb-IX-V leads to an intrinsic platelet defect was also supported by previous work in a mouse model with GPIb-IX-V mutations showing that an increased affinity for normal vWF (platelet-type vWD) was associated with a defect in platelet activation (17). Based on these 2 previous observations, we decided to undertake a comprehensive analysis of platelet functions in vWD-type 2B.

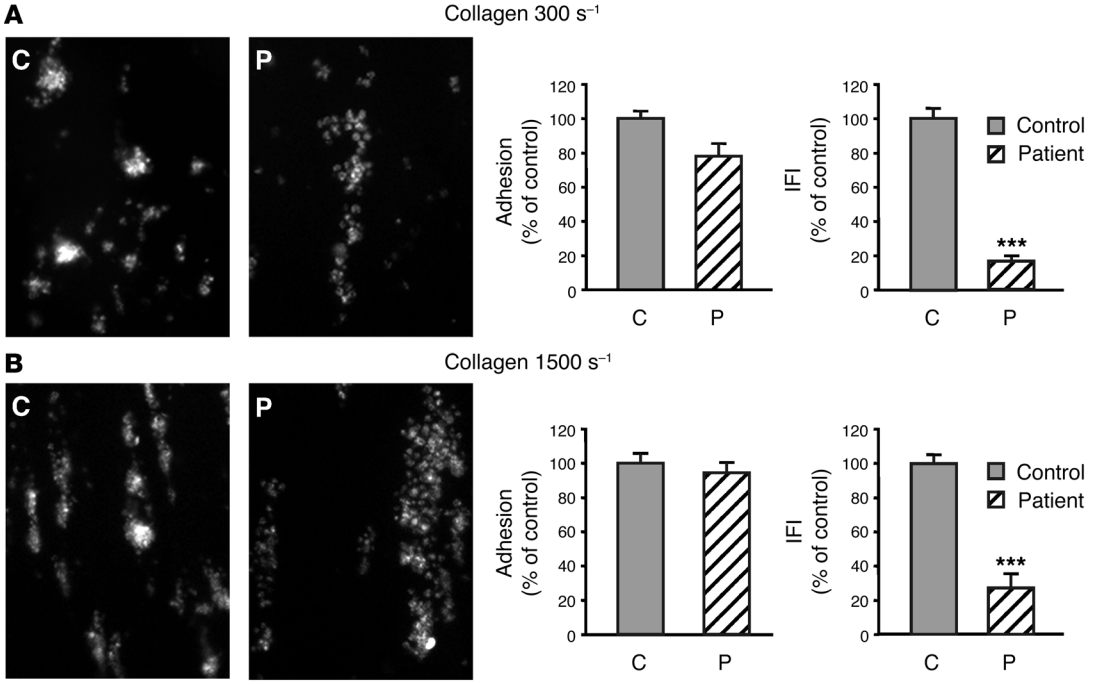

Figure 6
Thrombus formation in the patient with vWD-type 2B. Whole blood was perfused at (**A**) 300 s^{-1} or (**B**) 1,500 s^{-1} in glass microcapillary tubes coated with type I collagen (100 μg/ml). After 5 minutes (300 s^{-1}) and 2 minutes (1,500 s^{-1}), platelet thrombi were observed under an epifluorescence microscope (original magnification, ×20). Total area covered by platelets and total integrated fluorescence intensity (IFI) from 1 experiment carried out in triplicate are presented as the mean ± SEM. ***$P < 0.001$ (unpaired Student's *t* test). Results are representative of 2 independent experiments.

Our study focused on the vWD-type 2B mutation p.V1316M, which is associated with a severe thrombocytopenia and bleeding, in both humans and mice (5, 11). Three different experimental models were compared: (a) a murine model for vWD-type 2B, in which the mvWF/p.V1316M mutation is expressed via hydrodynamic injection (11, 18); (b) analysis of platelets isolated from a patient with vWD-type 2B heterozygous for the p.V1316M mutation; and finally, (c) a model in which isolated normal human platelets are activated after preincubation with recombinant hvWF/p.V1316M.

Platelets from mice expressing the p.V1316M mutation and from the patient with vWD-type 2B exhibiting the same mutation as well as control platelets preincubated with hvWF/p.V1316M all exhibited severely altered activation, through collagen receptors or GPCRs (thrombin or ADP receptors). αIIbβ3 activation was strongly impaired, leading to altered aggregation, secretion, and spreading of washed mouse platelets. Importantly, similar results were obtained with patient's platelets or with control platelets in the presence of recombinant hvWF/p.V1316M. Of note, aggregation and secretion defects for 2 patients with vWD-type 2B have been previously reported to be correlated with impaired granule contents (9). In our case, increase of granule contents (vWF and PF-4) and of receptors (αIIbβ3, β1, GPIbα, and GPVI) (around 150% of control) of the patient's platelets argues in favor of a specific signaling defect independent of the granule content and responsible for altered platelet function. This hypothesis is confirmed by all the experiments done in the presence of apyrase or antagonists of ADP receptors showing a specific effect on GPCRs and GPVI.

In blood flow experiments, the patient's platelets adhered to a collagen matrix at 300 s^{-1} but did not form thrombi, consistent with the absence of αIIbβ3 integrin engagement and with our in

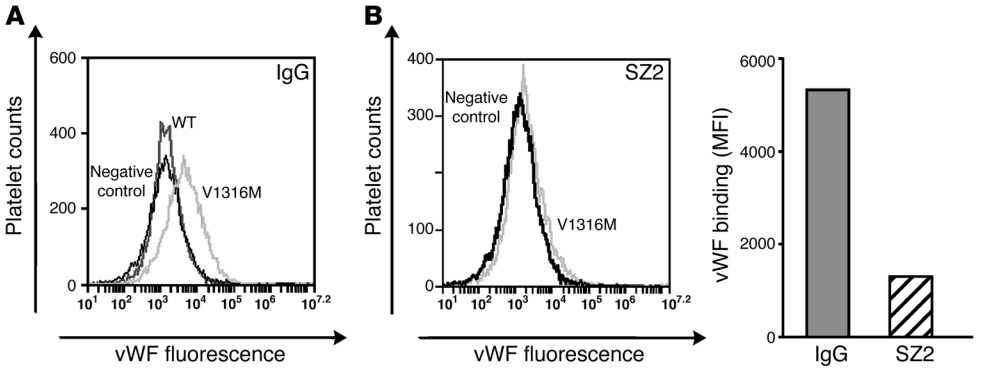

Figure 7
Binding of recombinant hvWF/p.V1316M to human control platelets. Binding of hvWF/p.V1316M or WT was monitored by flow cytometry using vWF polyclonal antibody. Human control platelet suspensions were pretreated for 5 minutes with (**A**) mouse IgG (10 μg/ml) or (**B**) GPIbα mAb (SZ2; 10 μg/ml) before addition of recombinant hvWF/p.V1316M or WT for 30 minutes. Results are representative of 3 independent experiments.

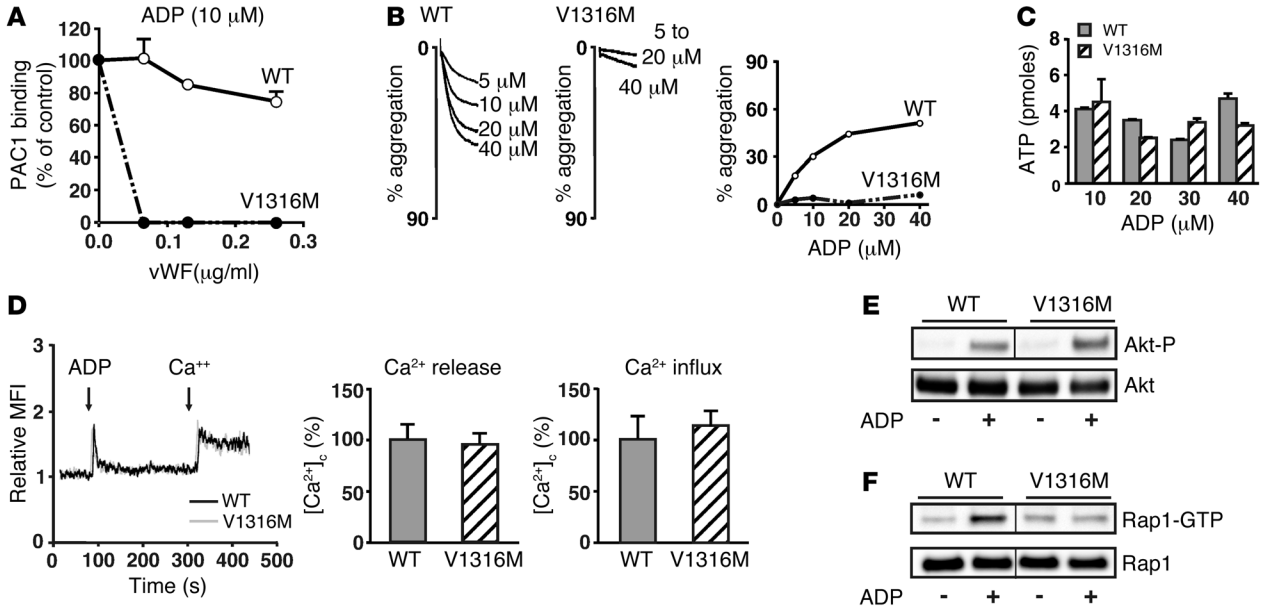

Figure 8

ADP-induced activation of human control platelets pretreated with recombinant hvWF/p.V1316M. Washed human control platelets pretreated for 10 minutes with recombinant hvWF/p.V1316M or WT were stimulated with ADP. (**A**) Integrin αIIbβ3 activation was assessed by flow cytometry using integrin αIIbβ3 mAb (PAC1) specific for the activated conformation of the human integrin. Data are mean ± SEM of 3 independent experiments carried out in triplicate. (**B**) Aggregation of washed platelets was initiated by adding various concentrations of ADP. (**C**) Dense granule secretion was assessed by measuring the amount of ATP release (pmoles). Data are mean ± SEM of 3 independent experiments carried out in triplicate. (**D**) Ca^{2+} signaling induced by 10 μM ADP was monitored by flow cytometry using the Oregon Green 488 BAPTA1-AM. Histograms represent the area under the curve of both Ca^{2+} store release and Ca^{2+} influx. Data from 1 experiment carried out in triplicate are presented as mean ± SEM. Results are representative of 2 independent experiments. (**E**) Akt-P after 5 minutes of stimulation with ADP (10 μM) in the absence of stirring was assessed by immunoblotting with anti–Akt-P. Total Akt and Akt-P blots were obtained by running equal amounts of sample on a parallel gel; the lanes of the Akt-P blot were derived from the same gel but were noncontiguous, as indicated by the black line. (**F**) Rap1 activity was measured by pull-down assay after 30 seconds of stimulation with ADP (10 μM) in the absence of stirring. The lanes of the blots were derived from the same gel but were noncontiguous, as indicated by the black lines. Results are representative of 3 independent experiments.

vitro finding of defective GPVI signaling. This defective activity of collagen receptors seems to be coupled to a defect in GPIb-IX-V–mediated platelet interaction with collagen-immobilized vWF, since at 1,500 s^{-1} no formation of thrombi was observed either. Whether this is the direct consequence of prior occupancy of GPIb-IX-V by mutant vWF (confirmed by our cell sorting experiments in the presence of a specific anti-GPIbα mAb) or secondary to defective αIIbβ3 activation is not known. The absence of thrombus formation at 1,500 s^{-1} thus confirms the defective interaction of GPIb-IX-V with immobilized vWF and subsequent defective signaling. Evidence for signaling directly induced by bound mutant vWF/p.V1316M comes from our observation that hvWF/p.V1316M induces the phosphorylation of Lyn in resting human control platelets in the absence of activation (results not shown). Lyn is usually activated by the interaction of WT-vWF with GPIb-IX-V in high shear conditions (19, 20). Conversely, the fact that platelet coverage was normal suggests strongly that impaired thrombus formation is a consequence of an integrin activation defect.

It is tempting to correlate the thrombus formation defect of the vWD/p.V1316M patient's platelets with the defect in αIIbβ3 activation upon stimulation of control platelets pretreated with recombinant hvWF/p.V1316M in the presence of ADP, thrombin, or Cvx (with or without apyrase). In these conditions, the defective Rap1 activation, a step critical for talin recruitment by integrin αIIbβ3 and its subsequent activation (21), appears to be a key mechanism to explain αIIbβ3 defective activation and engagement. This stands out even more strikingly in view of the fact that GPCR-dependent pathways (PLCβ), GPVI-dependent pathways (Syk, PLCγ2), and the shared Ca^{2+} release from intracellular stores required for activation of Rap1 were not affected. Therefore, our contention is that vWF/p.V1316M affects the activation pathway(s) of Rap1 but does so downstream of Ca^{2+} store release. Rap1 activity in platelets is controlled by 2 sets of proteins: (a) the guanine nucleotide exchange factors (GEFs) that stimulate the release of GDP and (b) the binding of GTP and the GTPases-activating proteins that stimulate the intrinsic Rap1 GTPase activity and restore the GDP-bound inactive state (22). The Ca^{2+}- and diacylglycerol-regulated CalDAG-GEF1 is the major regulator of Rap1 activation (23). Recently, CalDAG-GEF1 was shown to be negatively regulated by PKA activation (24). In our model of control platelets with vWF/p.V1316M, PKA pharmacological inhibition did not restore PAC1 binding induced by ADP or thrombin (results not shown), suggesting that PKA activation acting on CalDAG-GEF1 is probably not involved in Rap1 inhibition. One discrepancy between platelets from the patient with vWD-type 2B and control platelets in the presence of vWF/p.V1316M is an inhibition of Ca^{2+} influx in the former and not the latter. One attractive hypothesis is that vWD-type 2B platelets exhibit intrinsic signaling defects, not only due to vWF/p.V1316M-altered signaling in platelets, but also as a possible consequence of altered platelet biogenesis by megakary-

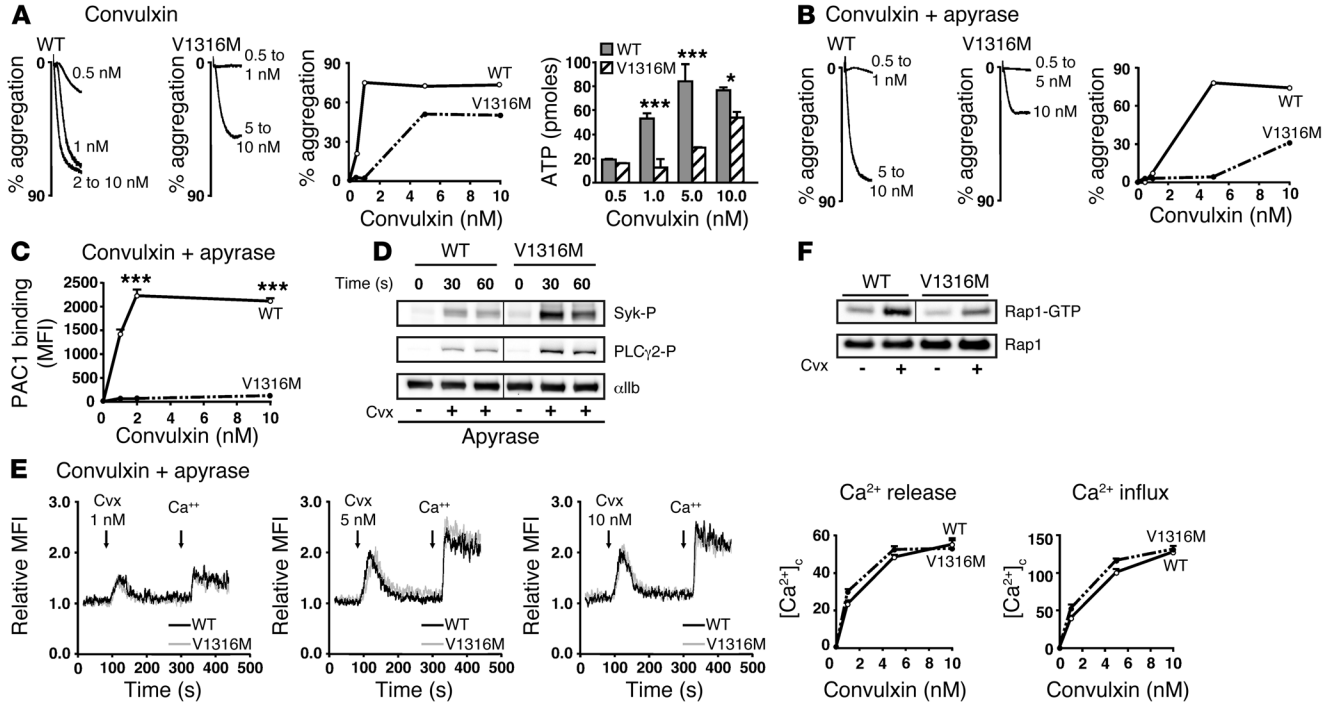

Figure 9

Cvx-induced activation of human control platelets pretreated with recombinant hvWF/p.V1316M. Washed human control platelets pretreated for 10 minutes with recombinant hvWF/p.V1316M or WT were stimulated with Cvx in the (**A**) absence or (**B**–**E**) presence of apyrase (2 U/ml) or (**F**) in the presence of antagonists of ADP receptors (AR-C69931MX, 10 μM; MRS 2179, 10 μM). (**A** and **B**) Aggregation and secretion of washed platelets were initiated by adding concentrations of thrombin (0.02–0.5 U/ml). Dense granule secretion was assessed by measuring the amount of ATP release. (**C**) Integrin αIIbβ3 activation induced by Cvx (1–10 nM) was assessed by flow cytometry using the integrin αIIbβ3 mAb PAC1 specific for the activated conformation of the human integrin. The level of activated integrin is indicated by MFI. (**D**) Washed platelets in suspension were activated by 4 nM Cvx for 30 and 60 seconds in the absence of stirring, and tyrosine Syk-P and PLCγ2-P was assessed by immunoblotting with anti–Syk-P and anti–PLCγ2-P, respectively. (**E**) Ca^{2+} signaling was monitored using Oregon Green 488 BAPTA1-AM. Curves represent the area under the curve of Ca^{2+} store release and Ca^{2+} influx. (**F**) Rap1 activity was measured by pull-down assay after 30 seconds of stimulation with Cvx (4 nM) in the absence of stirring and identified by immunoblotting with anti-Rap1 antibody. The presence of comparable amounts of Rap1 in aliquots of the all platelet samples is shown in a parallel gel; lanes of the Rap1-GTP blot were derived from the same gel but were noncontiguous, as indicated by the black line. Data from 1 experiment carried out in triplicate are presented as mean ± SEM. $^*P < 0.05$, $^{***}P < 0.001$ (unpaired Student's *t* test). Results are representative of 3 independent experiments.

ocytes leading to a defect in Ca^{2+} influx, for example, by altered expression and/or function of store-operated Ca^{2+} channels.

In conclusion, our study clearly demonstrates that vWF/p.V1316M alters platelet signaling, leading to inhibition of αIIbβ3 activation as well as platelet aggregation and thrombus formation. Such an impairment contributes to an as yet unrecognized thrombocytopathy that could contribute to the bleeding tendency observed with these patients.

Methods

Material. Equine type I collagen and ADP were obtained from Kordia. The PAR4-AP (AYPGKF-NH_2) was purchased from Bachem. Cvx and mAb directed against GPVI were provided by M. Jandrot Perrus (Inserm UMR 698, Paris 7-Denis Diderot University, CHU-X Bichat, Paris, France). Fibrinogen and polyclonal antibody directed against PF-4 were obtained from HYPHEN BioMed SAS. D-Phe-Pro-Arg chlormethylketone dihydrochloride (PPACK) was from Calbiochem-VWR. Apyrase grade VII, bovine thrombin, prostaglandin E_1, and rhodamin-6G were from Sigma-Aldrich. AR-C69931MX and MRS 2179 were provided by C. Gachet (Inserm UMR S949, Université de Strasbourg, EFS-Alsace, Strasbourg, France). The ATP Determination Kit, Oregon Green 488 BAPTA1-AM, Alexa Fluor 488–labeled phalloidin, and Fibrinogen Oregon Green 488 conjugate were from Molecular Probes. FITC-labeled PAC1, a ligand-mimetic integrin αIIbβ3–specific mAb that binds specifically to activated αIIbβ3, αIIbβ3-FITC, β1-PE, GPIbα-FITC, was purchased from Becton Dickinson. The polyclonal antibody directed against phosphorylated forms of Syk and PLCγ2 was obtained from Cell Signaling Technology. Phycoerythrin-labeled rat anti-mouse mAb that binds specifically to activated integrin αIIbβ3 (JON/A) and FITC-labeled rat anti-mouse CD62P (P-selectin) mAb (Wug.E9) were obtained from Emfret Analytics. RalGDS-RBD coupled to agarose beads was purchased from Millipore. Polyclonal antibody directed against Rap1A/1B was obtained from Cell Signaling Technology. The polyclonal antibody directed against human vWF was from DAKO, and the mAb directed against GPIb (clone SZ2) was from Beckman Coulter.

Mouse strains. vWF-deficient mice were backcrossed onto a C57BL/6 background for more than 12 generations, yielding congenic C57BL/6 *Vwf*$^{-/-}$ mice. All experimental procedures were carried out in accordance with the European legislation concerning the use of laboratory animals and approved by the Animal Care and Ethical Committee of Université Paris-Sud.

Hydrodynamic injection. To study vWD-type 2B mutation in murine vWF, mice were injected with pLIVE-mvWF encoding WT-mvWF and

pLIVE-mvWF/V1316M plasmids (25–30 μg) using the hydrodynamic injection method, as described previously (11). After 4 days, blood was collected. Compared with normal pooled mouse plasma (100%), average antigen levels were 1,016.7% ± 86.6% and 598.3% ± 65.3% for WT-mvWF and mvWF/p.V1316M-expressing mice, respectively. No vWF was detected in α granules. Moreover, mutation was associated with a severe thrombocytopenia (mvWF/p.V1316M, 169 ± 16 × 10^9 platelets per l) and increased platelet volume (mvWF/p.V1316M, 6.8 ± 0.06 μm^2) compared with WT-mvWF (5.1 ± 0.04 μm^2) mice. Bleeding tendency measured by a tail bleeding test was explored in a previous report (11). After 4 days, WT-mvWF–expressing mice stopped bleeding within 2 minutes, whereas the bleeding time for mvWF/p.V1316M mice was largely increased, exceeding the 10-minute observation period (11). Thrombus formation in a ferric chloride–induced thrombosis model was also addressed at day 4 in a previous study (11). While WT-mvWF allowed occlusion of venous and arterial mesenteric vessels, mvWF/p.V1316M was associated with a severe deficiencies in thrombus formation.

Recombinant hvWF/p.V1316M. Baby hamster kidney cells were transfected with pNUT-hvWF and pNUT-hvWF/p.V1316M encoding hvWF and hvWF/p.V1316M as previously described (11). Serum-free–conditioned medium was collected, and vWF antigen levels were quantified, taking normal pooled human plasma as a reference (100%).

Blood collection and mouse platelet preparation. Mice were anesthetized with tribromoethanol 2.5% and blood was collected from the retroorbital venous plexus in 10% (vol/vol) ACD-C buffer (124 mM sodium citrate, 130 mM citric acid, 110 mM dextrose, pH 6.5). Isolated platelets were obtained as previously described (25).

Patient and platelet preparation. One patient with *vWF* mutation associated with vWD-type 2B was enrolled in this study after informed consent and in accordance with the Declaration of Helsinki. The patient is a man with mutation corresponded to a p.Val1316Met (V1316M) substitution. The bleeding score was high (14) and associated with a severe history of bleeding (epitaxis, hematomas, gum bleeding) and a low platelet count (40 × 10^9 platelets per l at the time of examination) (Table 1). Complete loss of high-molecular-weight multimers was observed.

Venous blood from the patient was collected in 10% (vol/vol) ACD-A buffer (75 mM trisodium citrate, 44 mM citric acid, 136 mM glucose, pH 4) for experiments with washed platelets (26). The blood sample was allowed to settle for 2 hours at room temperature in 5-ml plastic tubes and then platelet-rich plasma (PRP) was collected. Enlarged platelets and small aggregates were detected in PRP (Supplemental Figure 2). Moreover, staining of unpermeabilized platelets with a rabbit anti-human vWF showed the presence of vWF/p.V1316M on platelet surface. Then, platelets were washed in the presence of apyrase (100 mU/ml) and prostaglandin E1 (1 μM) to minimize platelet activation. The numbers of patient and control platelets were adjusted to similar levels (2.5 × 10^8 platelets per ml) in Tyrode buffer (137 mM NaCl, 2 mM KCl, 0.3 mM NaH_2PO_4, 1 mM $MgCl_2$, 5.5 mM glucose, 5 mM N-2-hydroxyethylpiperazine-N′-2-ethanesulfonic acid, 12 mM $NaHCO_3$, 2 mM $CaCL_2$, pH 7.3).

Platelet aggregation. The low platelet count obtained in the patient's PRP (40 × 10^9 platelets per l) prevented its use for platelet aggregation. Therefore, platelet aggregation was carried out with washed platelets induced by GPCR agonists (ADP, thrombin, PAR1-AP, and PAR4-AP), Cvx, and collagen. Indeed, Cvx has been shown to bind not only GPVI but also GPIb (27). Light transmission was measured through the stirred suspension of platelets (2.5 × 10^8 platelets per ml) for 3 minutes using a Chronolog aggregometer (Coultronics) (25).

Platelet dense granule secretion. Dense granule secretion was quantified by measuring ATP release during platelet aggregation using a luminometer (Fluostar Optima; BMG Labtech) as previously described (25).

Flow cytometric analysis. Platelets were stimulated with a range of agonists for 15 minutes and then incubated with various fluorophore-conjugated antibodies. Samples were analyzed in an Accuri C6 (Becton Dickinson) flow cytometer.

Immunoblotting. Washed platelets (2.5 × 10^8 platelets per ml; 300 μl) were stimulated with Cvx (4 nM) and apyrase (2 U/ml) in the absence of stirring. After 3 minutes, the platelets were lysed in SDS denaturing buffer (50 mM Tris, 100 mM NaCl, 50 mM NaF, 5 mM EDTA, 40 mM β-glycerophosphate, 100 μM phenylarsine oxide, 1% SDS, 5 μg/ml leupeptin, 10 μg/ml aprotinin, pH 7.4). The proteins were subjected to SDS-PAGE and transferred to nitrocellulose. The membranes were incubated with various primary antibodies (see Results). Immunoreactive bands were visualized using Enhanced Chemiluminescence Detection Reagents (Pierce). Images of the chemiluminescent signal were captured using G:BOX Chemi XT16 Image Systems and quantified using Gene Tools version 4.0.0.0 (Syngene).

Measurement of intracellular free calcium concentration. Human control platelets (2 × 10^7 platelets per ml) were loaded with the Ca^{2+}-sensitive dye Oregon Green 488 BAPTA1-AM (1 mM) for 45 minutes at 20°C. After pretreatment of the control platelets for 10 minutes with recombinant hvWF mutants, Ca^{2+} mobilization induced by agonists (ADP, PAR4-AP, and Cvx) was analyzed in Ca^{2+}-free medium using an Accuri C6 (Becton Dickinson) flow cytometer. Ca^{2+} influx was later induced by adding Ca^{2+} (200 μM) in extracellular medium.

Rap1 pull-down assay. Unstirred platelets were stimulated for 30 seconds. Rap1-GTP was pulled down from lysates using RalGDS-RBD beads as described previously (28).

Thrombus formation under flow. Blood was collected in PPACK (80 μM) for flow experiments, and platelet counts in blood were normalized. Blood perfusion experiments were performed on a fibrillar collagen matrix at 2 shear rates (300 s^{-1} and 1,500 s^{-1}). Glass coverslips were coated with collagen (100 μg/ml) overnight at 4°C. Briefly, blood samples were labeled with rhodamine 6G (10 μg/ml) for 5 minutes at 37°C and then perfused for 5 minutes (300 s^{-1}) and 2 minutes (1,500 s^{-1}) with a syringe pump (Fisher Scientific) (25). Real-time thrombus formation was recorded with an inverted epifluorescence microscope (Nikon Eclipse TE2000-U) coupled to Metamorph 7.0r1 software (Universal Imaging Corporation). Thrombus formation was quantitated by assessment of the mean percentage of the total area covered by thrombi and by the mean of integrated fluorescence intensity per square micron of each thrombus (29).

Statistics. Results were analyzed using the 2-tailed Student's *t* test as indicated. A *P* value of less than 0.05 was considered significant.

Study approval. Patients gave written informed consent before participating in this study and were enrolled in the study in accordance with the Declaration of Helsinki. Animals experiments adhered to protocols approved by ethical committee of Université Paris-Sud (CEEA26; 2012:039).

Acknowledgments

The authors wish to thank the patient who participated in this study. This study was financially supported by grants from INSERM and Agence Nationale de la Recherche (ANR 11 BSV1 010 01 to C.V. Denis) and Fondation pour la Recherche Médicale (SPF20101220866).

Received for publication July 18, 2013, and accepted in revised form September 9, 2013.

Address correspondence to: Marijke Bryckaert, INSERM U770 Hôpital Bicêtre, 80 rue du Général Leclerc, 94276 Le Kremlin Bicêtre Cedex, France. Phone: 33.149595642; Fax: 33.146719472; E-mail: marijke.bryckaert@inserm.fr.

1. Ruggeri ZM. Von Willebrand factor: looking back and looking forward. *Thromb Haemost*. 2007; 98(1):55–62.
2. Sadler JE. Von Willebrand factor, ADAMTS13, and thrombotic thrombocytopenic purpura. *Blood*. 2008;112(1):11–18.
3. Ginsburg D, Bowie EJ. Molecular genetics of von Willebrand disease. *Blood*. 1992; 79(10):2507–2519.
4. Ginsburg D, Sadler JE. von Willebrand disease: a database of point mutations, insertions, and deletions. For the Consortium on von Willebrand Factor Mutations and Polymorphisms, and the Subcommittee on von Willebrand Factor of the Scientific and Standardization Committee of the International Society on Thrombosis and Haemostasis. *Thromb Haemost*. 1993;69(2):177–184.
5. Federici AB, et al. Clinical and molecular predictors of thrombocytopenia and risk of bleeding in patients with von Willebrand disease type 2B: a cohort study of 67 patients. *Blood*. 2009; 113(3):526–534.
6. Sadler JE, et al. Update on the pathophysiology and classification of von Willebrand disease: a report of the Subcommittee on von Willebrand Factor. *J Thromb Haemost*. 2006;4(10):2103–2114.
7. Nurden P, et al. Abnormal VWF modifies megakaryocytopoiesis: studies of platelets and megakaryocyte cultures from patients with von Willebrand disease type 2B. *Blood*. 2010; 115(13):2649–2656.
8. Saba HI, Saba SR, Dent J, Ruggeri ZM, Zimmerman TS. Type IIB Tampa: a variant of von Willebrand disease with chronic thrombocytopenia, circulating platelet aggregates, and spontaneous platelet aggregation. *Blood*. 1985;66(2):282–286.
9. Lopez-Fernandez MF, et al. Type IIB von Willebrand's disease associated with a complex thrombocytopenic thrombocytopathy. *Am J Hematol*. 1988;27(4):291–298.
10. Sugimoto M, et al. Mural thrombus generation in type 2A and 2B von Willebrand disease under flow conditions. *Blood*. 2003;101(3):915–920.
11. Rayes J, et al. Mutation and ADAMTS13-dependent modulation of disease severity in a mouse model for von Willebrand disease type 2B. *Blood*. 2010; 115(23):4870–4877.
12. Varga-Szabo D, Braun A, Nieswandt B. Calcium signaling in platelets. *J Thromb Haemost*. 2009; 7(7):1057–1066.
13. Bunescu A, et al. Partial expression of GP Ib measured by flow cytometry in two patients with Bernard-Soulier syndrome. *Thromb Res*. 1994; 76(5):441–450.
14. Cosemans JM, Munnix IC, Wetzker R, Heller R, Jackson SP, Heemskerk JW. Continuous signaling via PI3K isoforms beta and gamma is required for platelet ADP receptor function in dynamic thrombus stabilization. *Blood*. 2006;108(9):3045–3052.
15. Rendal E, et al. Type 2B von Willebrand's disease due to Val1316Met mutation. Heterogeneity in the same sibship. *Ann Hematol*. 2001; 80(6):354–360.
16. Morowski M, Vogtle T, Kraft P, Kleinschnitz C, Stoll G, Nieswandt B. Only severe thrombocytopenia results in bleeding and defective thrombus formation in mice. *Blood*. 2013;121(24):4938–4947.
17. Guerrero JA, et al. Visualizing the von Willebrand factor/glycoprotein Ib-IX axis with a platelet-type von Willebrand disease mutation. *Blood*. 2009; 114(27):5541–5546.
18. Golder M, et al. Mutation-specific hemostatic variability in mice expressing common type 2B von Willebrand disease substitutions. *Blood*. 2010; 115(23):4862–4869.
19. Yin H, Liu J, Li Z, Berndt MC, Lowell CA, Du X. Src family tyrosine kinase Lyn mediates VWF/GPIb-IX-induced platelet activation via the cGMP signaling pathway. *Blood*. 2008;112(4):1139–1146.
20. Suzuki-Inoue K, et al. Glycoproteins VI and Ib-IX-V stimulate tyrosine phosphorylation of tyrosine kinase Syk and phospholipase Cgamma2 at distinct sites. *Biochem J*. 2004;378(pt 3):1023–1029.
21. Nieswandt B, et al. Loss of talin1 in platelets abrogates integrin activation, platelet aggregation, and thrombus formation in vitro and in vivo. *J Exp Med*. 2007;204(13):3113–3118.
22. Zwartkruis FJ, Bos JL. Ras and Rap1: two highly related small GTPases with distinct function. *Exp Cell Res*. 1999;253(1):157–165.
23. Stefanini L, Roden RC, Bergmeier W. CalDAG-GEFI is at the nexus of calcium-dependent platelet activation. *Blood*. 2009;114(12):2506–2514.
24. Guidetti GF, Manganaro D, Consonni A, Canobbio I, Balduini C, Torti M. Phosphorylation of the guanine-nucleotide exchange factor CalDAG-GEFI by protein kinase A regulates Ca2+-dependent activation of platelet Rap1b GTPase. *Biochem J*. 2013; 453(1):115–123.
25. Adam F, et al. Platelet JNK1 is involved in secretion and thrombus formation. *Blood*. 2010; 115(20):4083–4092.
26. Kauskot A, et al. Involvement of the mitogen-activated protein kinase c-Jun NH2-terminal kinase 1 in thrombus formation. *J Biol Chem*. 2007; 282(44):31990–31999.
27. Kanaji S, Kanaji T, Furihata K, Kato K, Ware JL, Kunicki TJ. Convulxin binds to native, human glycoprotein Ib α. *J Biol Chem*. 2003; 278(41):39452–39460.
28. Crittenden JR, et al. CalDAG-GEFI integrates signaling for platelet aggregation and thrombus formation. *Nat Med*. 2004;10(9):982–986.
29. Braun A, et al. Orai1 (CRACM1) is the platelet SOC channel and essential for pathological thrombus formation. *Blood*. 2009; 113(9):2056–2063.